Seatific, Vol. 2, Issue. 1, pp. 52–72, June 2022

Seatific
https://seatific.yildiz.edu.tr
DOI: https://doi.org/10.14744/seatific.2022.0005

Research Article

Performance evaluation of spectral wave model forced by ERA-Interim, ERA5, and CFSR wind fields in the Black Sea

Fulya İşlek*, Yalçın Yüksel, Adem Özdemir

Department of Civil Engineering, Yıldız Technical University, İstanbul, Türkiye

ARTICLE INFO

Article history
Received: May 23, 2022
Revised: June 16, 2022
Accepted: June 29, 2022

Key words:
Black Sea; CFSR; ERA5; ERA-Interim; MIKE 21 SW; Wave model calibration

ABSTRACT

The main objective of the present study is to evaluate the performance of the MIKE 21 SW (Spectral Wave) in a semi-closed basin (Black Sea). Wind data were obtained from the European Centre for Medium-Range Weather Forecasts (ECMWF) ERA-Interim, ECMWF ERA5, and the National Centers for Environmental Prediction (NCEP) Climate Forecast System Reanalysis (CFSR) datasets. The wave model was calibrated and validated with wave measurements recorded at seven different stations along the Black Sea coastlines. During the calibration, several different physical parameters were tested to determine the optimal model settings, with the whitecapping parameter (C_{ds}) being more influential than the bottom friction parameter (k_n), wave breaking parameter (γ), and nonlinear wave-wave interactions in the prediction of the Black Sea wave properties. The wave results modeled using ERA-Interim showed less agreement with wave measurements than those obtained with ERA-5 and CFSR wind fields. Although the significant wave height and wave period modeled using ERA5 and CFSR wind fields were reasonably well matched at all measurement stations, ERA5 wind fields provided slightly better performance owing to having the largest correlation coefficient (R) and lowest statistical error measures (bias, RMSE, SI) in the Black Sea.

Cite this article as: İşlek F, Yüksel Y, Özdemir A. Performance evaluation of spectral wave model forced by ERA-Interim, ERA5, and CFSR wind fields in the Black Sea. Seatific 2022;2:1:52–72.

1. INTRODUCTION

Long-term wave climate analyses under both normal and extreme conditions, wave power assessments, future wave climate assessments, and studies into possible climate change impacts in the semi-enclosed sea areas such as the Adriatic Sea (Cavaleri et al., 2018), Baltic Sea (Soomere and Raamet, 2011), Black Sea (Islek and Yuksel 2021; Islek et al., 2021), Sea of Marmara (Yuksel et al., 2021), Caspian Sea (Onea et al., 2015), Mediterranean Sea (Yuksel et al., 2020) are more challenging compared to open seas. In these marine regions, there are several affecting factors including the presence of land-associated orography and extended areas of shallow waters (Cavaleri et al., 2018). Moreover, the wave climate is one of the most sensitive indicators of changes in the wind regime and local climate in the semi-enclosed sea areas (Weisse and von Storch, 2010).

The present study focuses on the Black Sea, which is one of the world's largest semi-enclosed basins. The basin has the variability of climatic and atmospheric circulation conditions (Siberian and Azores anticyclones) and is surrounded by complex orography (wind shadow effect

***Corresponding author.**
*E-mail address: islek.fulya@gmail.com

related to the influence of high mountains surrounding the basin). Another important feature of the basin is that the western shelf is narrower than the northeastern shelf but wider than the rest of the Black Sea (Valchev et al., 2010). The Black Sea basin is roughly divided into two main zones (i.e., west, and east) in terms of wind/wave characteristics and wind/wave power (Divinsky and Kosyan 2017; Islek et al., 2020a, and 2020b). Due to having complex and complicated wind/wave characteristics, the Black Sea basin always requires having knowledge of reliable wave hindcasts (Islek et al., 2020a). Various spectral wave models were used to model wave characteristics in the Black Sea:

Valchev et al. (2013) used the WAM model forced with the wind output of the regional atmospheric model REMO to assess the offshore wave energy in a 59-year (1948-2006) period. Divinsky and Kosyan (2015) examined the wave climate tendencies in a 25-year (1990-2014) period using the two spectral wave models, i.e., MIKE 21 SW (Spectral Wave) and SWAN (Simulating WAves Nearshore). The researchers reported that both models performed similar and comparable results. Then, the researchers (Divinsky and Kosyan, 2017) used the MIKE 21 SW model to investigate the spatiotemporal variability of the Black Sea wave climate for the 37-year ERA-Interim wind fields (1979-2015). The performance of wind-wave modeling was evaluated by Rusu et al. (2014) and the two models were used: WRF (Weather Research and Forecasting) for wind and SWAN for waves. A 40-year ERA-Interim and CFSR (Climate Forecast System Reanalysis) wind fields (1979-2018) were utilized to force the MIKE 21 SW model by Islek et al. (2020b) and to force the SWAN model by Islek et al. (2021). In both studies, the researchers investigated the long-term variations of wave characteristics. Myslenkov et al. (2021) used Wavewatch III and SWAN models using GFS (Global Forecasting System) of NCEP (National Centers for Environmental Prediction) and COSMO-RU07 (Consortium for the small-scale modeling-Russian domain for 7 km) forcing.

It is important to note that the accuracy of the wave model mainly depends on the quality of wind forcing fields, primarily wind speed data (Cavaleri and Bertotti, 2006; Rusu et al., 2014; Islek et al., 2020a; Myslenkov et al., 2021). The previous studies agree that using high-quality wind fields as input data improves the accuracy of wave models. Several studies have been carried out in the Black Sea to compare the SWAN model performance forced with different wind sources; ECMWF (European Centre for Medium-Range Weather Forecast) Operational, ERA40, CFSR, MERRA (Modern-ERA Retrospective Analysis), JRA-25 (Japanese 25-year reanalysis) by Van Vledder and Akpinar (2015), CFSR, GFS forecast, and WRF reanalysis and forecast by Myslenkov et al. (2016); CFSR, ERA-Interim, and MERRA winds by Akpinar and Ponce de Leon (2016), ERA-Interim and CFSR by Islek et al. (2021) and Islek and Yuksel (2021). However, there is a limited number of studies on the MIKE 21 SW model performance using different wind sources. Moreover, the accuracy of wave results modeled using ERA5 reanalysis wind data, which is the most up-to-date reanalysis dataset, and its contribution to wave model performance are fully unknown.

In the present study, we aimed to determine the effect of different wind sources on MIKE 21 SW model performance in a semi-closed basin, the Black Sea. For this purpose, wave characteristics were simulated using the three wind fields with different spatial and temporal resolutions (namely, ERA-Interim, ERA5, and CFSR). Model results were calibrated and validated by comparing wave measurements obtained from the seven different measurement stations along the Black Sea and model performance forced by the three different wind fields was assessed using statistical error measures for quantitative comparison.

2. MATERIALS AND METHODS

In this study, the performance of the MIKE 21 SW model in the Black Sea was evaluated using the three different wind sources (ERA-Interim, ERA5, CFSR). All the wind fields contain horizontal wind components at 10 m above the sea surface.

ERA-Interim (hereafter ERA-I) reanalysis dataset (Dee et al., 2011) is provided by ECMWF online data server from 01/01/1979 to 31/08/2019. ERA-I is derived from a more advanced assimilation system (4D variational assimilation) than ERA40, which uses 3D variational assimilation. The assimilation system is based on the Integrated Forecasting System (IFS, Cycle 41r2). ERA-I reanalysis dataset has a 6-h temporal resolution and a ~79 km (0.75°×0.75°) spatial resolution from the native T255 spectral grid. The dataset resolves the atmosphere using 60 levels from the surface up to 0.1 hPa.

ERA5 (Hersbach et al., 2016) is the fifth-generation climate reanalysis from the ECMWF and has replaced ERA-I. Because the recent reanalysis has many significant improvements compared to ERA-I, e.g., ERA5; (i) has longer datasets covering the data from 1950 to present, (ii) provides an enhanced horizontal resolution of a ~31 km (0.75°×0.75°) from native T636 spectral grid, (ii) provide higher temporal resolution, (iii) resolves the atmosphere using 137 levels from the surface up to 0.01 hPa (~80 km), (iv) uses the 4D-Var data assimilation using IFS Cycle 41r2 instead of IFS Cycle 31r2 in ERA-I, (v) has enhanced the number of output parameters, (vi) include an uncertainty estimate. Detailed information can be found in (Hersbach et al., 2016). It is important to note that, the performance of the wave model forced with the new ERA5 reanalysis wind data is not fully known.

The NCEP CFSR (Saha et al. 2010) and CFSv2 (Saha et al. 2014) reanalysis datasets cover the periods of 1979-2010 and 2011-present, respectively. Both versions are derived by a

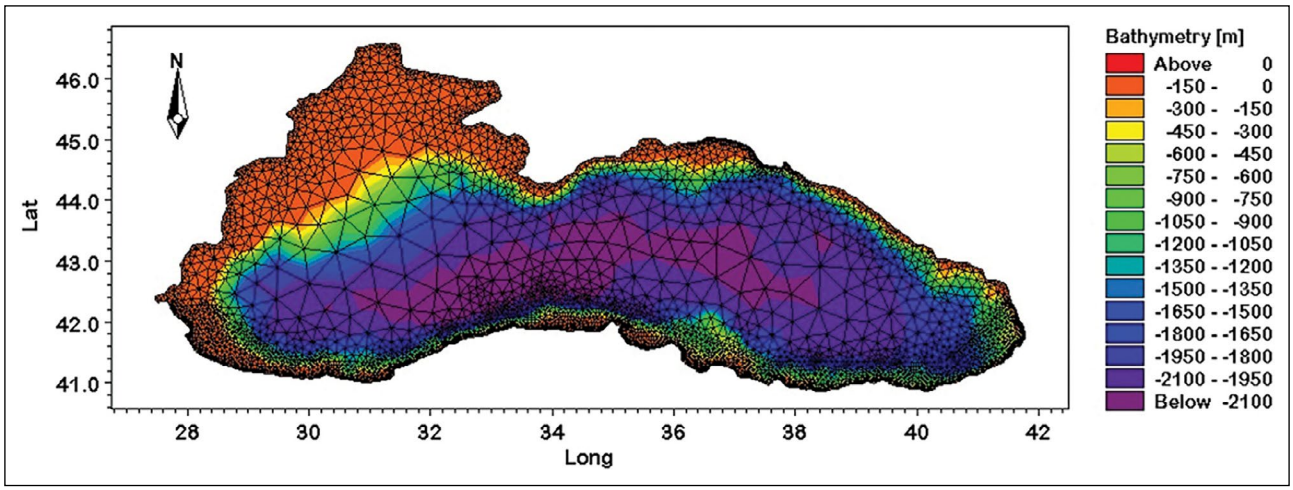

Figure 1. Computational mesh and bathymetry of the Black Sea.

3D variational assimilation system and use the same model. However, CFSv2 dataset is improved with higher horizontal and vertical resolutions and intensive use of satellite observations. CFSR dataset provides different resolutions in version 1 ranging from 0.312°×0.312° to 2.5°×2.5° and version 2 between 0.205°×0.205° and 2.5°×2.5°, respectively. Both versions provide the dataset with a temporal resolution of 1 h. To ensure consistency between the two versions, the spatial resolution of 0.5°×0.5° was selected, which is the finest resolution provided in both versions.

In the present study, ERA-I and ERA5 were downloaded with a spatial resolution of 0.25°x0.25° in both longitude and latitude, and temporal resolutions of 6-h and 1-h, respectively. CFSR wind fields with a 1-h temporal resolution and a spatial resolution of 0.5°×0.5° in both longitude and latitude. ERA5 and CFSR datasets considered in this study have the same temporal resolution (1 h), while ERA5 dataset provides a finer spatial resolution compared to CFSR and ERA-I.

3. MODEL SETUP

In this study, the third-generation spectral wave model MIKE 21 SW developed by Danish Hydraulic Institute (DHI, 2007) is used to generate the wave fields in the Black Sea. The model is based on a fully spectral formulation with parameterization of the wave action conservation equation (Holthuijsen et al., 1989). It simulates the growth, decay, and transformation of wind-generated waves and swells in offshore and coastal areas. A detailed description of the MIKE 21 SW model can be found in the DHI (2007).

The first step in each MIKE 21 SW simulation is to define the computational domain for the Black Sea model area. An unstructured mesh technique was used, which enables boundary-fitted flexible meshing. To get more accurate wave results, the finer mesh was implemented in the coastal areas and coarser offshore. To determine the optimal values of computational mesh, the model runs different mesh alternatives. Considering the computational time, hard disk storage (since the wave parameters of the domain are calculated based on the nodes of the computational mesh), and correlation coefficient of the results, a two-dimensional triangular computational mesh was generated. The Mesh Generator module of MIKE Zero was used (DHI, 2007). The final mesh consists of 4755 nodes and 8213 triangular elements for the Black Sea shown in Figure 1.

After the computational domain was determined, bathymetric data and wind fields were identified for each simulation. The bathymetric data of the Black Sea were obtained from the Turkish Naval Forces Office of Navigation, Hydrology, and Oceanography (ONHO) and was interpolated onto the computational mesh. Two-dimensional triangular computational mesh and bathymetry of the Black Sea are depicted in Figure 1. The wind fields that were used as input in this study were provided from ECMWF ERA-Interim, ECMWF ERA5, and NCEP CFSR datasets.

Lastly, important physical processes such as generation and growth of wind waves, non-linear wave-wave interaction, dissipation due to whitecapping, bottom friction, and depth-induced wave breaking, refraction, diffraction, and shoaling of the waves during the propagation were considered in the modeling study. During the determination of the optimal model settings, model meshes with different resolutions and different spectral and directional discretization were tested and the best fit between the modeled and measured wave parameters was investigated.

To determine the best agreement between the MIKE 21 SW model hindcasts and wave measurements, numerous calibration tests were conducted by tuning the whitecapping parameter (C_{ds}), the wave breaking parameter (γ), the bottom friction parameter (k_n), and the consideration of

Table 1. Physical processes in the spectral wave model

Energy source term	Physical process	Formulation/source
Input (S_{in})	The growth of waves	Komen et al. (1994)
Wave energy dissipation ($S_{ds}+S_{bot}+S_{surf}$)	Whitecapping	Komen et al. (1994) C_{ds}=0.5–2.0 varying with wind input, δ=0.5
	Bottom friction	Constant Nikuradse roughness k_n=0.04 m
	Wave breaking	Battjes and Janssen (1978) α=1, γ=0.8
Nonlinear wave-wave interactions (S_{nl})	Quadruplet wave interactions	Discrete Interaction Approximation (DIA) by Hasselman et al. (1985)
	Triad wave interactions	Opt-out

Table 2. Characteristics of the measurement stations in the Black Sea

Station name	Coordinates (°)	Depth (m)	Data period	Measured wave data	Source
Gelendzhik	44°30'27" N 37°58'42" E	-85	01.07.1996–10.12.2003	H_s, T_m	Ozhan and Abdalla (2002)
Hopa	41°25'24" N, 41°23'00" E	-100	21.12.1994–30.04.1999	H_s, T_m	Ozhan and Abdalla (2002)
Sinop	42°07'24" N, 35°05'12" E	-100	01.11.1994–20.06.1996	H_s, T_m	
Filyos	41°60'00'' N, 32°02'00'' E	-100	21.12.1994–26.12.1996	H_s, T_p	DLH (1999)
Karaburun	41°21'00" N 28°41'00" E	-16	30.08.2003–17.12.2004	H_s, T_m	Ari Guner et al. (2013)
Samsun	41°26'14" N, 36°28'30" E	-280	09.03.2015–20.03.2016	H_s, T_m	Turkish State Meteorological Service (TSMS)
Bosphorus	41°17'32" N, 29°09'56" E	-95	11.03.2016–19.11.2018	H_s, T_p	TSMS

triad wave interactions. The optimal values of physical model parameters are summarized in Table 1. The following formulations gave the best wave results: the wind formulation was used proposed by Komen et al. (1994) which calculates a coupled wind-sea dependent roughness. The expression of Komen et al. (1994) was considered for wave energy dissipation due to whitecapping. Constant Nikuradse roughness k_n with 0.04 m was used for bottom friction. The formulation based on the bore model by Battjes and Janssen (1978) with α=1 and γ=0.8 was used for wave energy dissipation by depth-limited wave breaking. Quadruplet-wave interaction was computed in the simulations using the Discrete Interaction Approximation (DIA) by Hasselmann et al. (1985). In the spectral space, the number of directions in the 360° rose was 16 directional bins. The frequency range was defined to be between 0.04 Hz and 1.0 Hz on a logarithmic scale and the number of frequencies was 25. The model was run with a calculation time step of 10 min and an output time step of 1 h.

Our results indicate that the whitecapping parameter (C_{ds}) is found to be a tunable parameter because the model simulations showed strong sensitivity to whitecapping dissipation simulations (Yuksel et al., 2020; Islek and Yuksel, 2021; Islek et al., 2021). Further calibration tests were performed in Section 4.1 to determine the value of a tunable parameter (whitecapping parameter C_{ds}) which gives a better estimation of the wave parameters and detailed validation results were given in Section 4.2.

4. RESULTS AND DISCUSSION

MIKE 21 SW model performance forced with the three different wind fields was evaluated to determine the effects of the wind fields with different spatial and temporal resolutions on the model performance. The model results were calibrated and validated by evaluating seven different measurement stations (Gelendzhik, Hopa, Sinop, Filyos, Karaburun, Samsun, and Bosphorus) along the Black Sea. The characteristics of the measurement stations are given in Table 2 and the locations of the stations are shown in Figure 2. In this study, the calibration and validation were made according to the peak wave period at Filyos,

Figure 2. Locations of the wave measurements stations in the Black Sea.

and Bosphorus stations, and the mean wave period was used at the other stations (Gelendzhik, Hopa, Sinop, Karaburun, and Samsun) for which the peak wave period measurements were not available.

4.1. Calibration evaluation in the Black Sea

The accuracy of the model results was calibrated using wave measurements including significant wave heights and wave periods at Gelendzhik, Hopa, Sinop, Filyos, and Karaburun stations (Fig. 2).

The calibration process was performed separately for the three different wind sources to detect the best agreement between the modeled and measured wave parameters in the Black Sea. Considering the optimal model settings given in Table 1, detailed calibration was performed by adjusting the whitecapping parameter (C_{ds}) with values ranging from 0.5 to 2.0. Scatter diagrams for modeled and measured wave results are depicted in Figure 3 for significant wave heights and Figure 4 for wave periods. To quantitatively evaluate the wave results, the statistical error measured are presented in Table 3 and Table 4 for significant wave heights and wave periods, respectively. Quantile-Quantile (Q-Q) plots to check the accuracy at the lowest/highest percentile can be seen in Appendix 1 and 2. The comparisons of time histories between modeled and measured significant wave heights and wave periods are given in Appendix 3-8.

In the Black Sea, the wave results modeled using ERA-I wind fields showed a significant variation in different values of the whitecapping parameter (C_{ds}) ranging from 0.5 to 2.0. The modeled wave results underestimated when the increasing C_{ds} from the value of 0.5. Moreover, ERA-I underestimated wave fields compared to wave results obtained from ERA5 and CFSR. An optimal accuracy with the lowest error (bias, RMSE, SI), and the largest correlation rates (R) between measured and modeled wave parameters were found with the value of C_{ds}=0.5 for ERA-I (Figs. 3, 4 and Tables 3, 4).

Using ERA5 wind fields, the statistical error results (Tables 3, 4) significantly increase when the reducing C_{ds} from the value of 1.5, and similar increasing statistical error results were detected when the increasing C_{ds} from the value of 1.5. Considering the statistical error results presented in Tables 3 and 4 and scatter diagrams shown in Figures 3 and 4, the modeled wave results obtained using C_{ds}=1.5 are in reasonably good agreement with the wave data measured at almost all stations. The performance of the MIKE 21 SW model forced with ERA5 gave more accurate wave results than those obtained with ERA-I. The difference may be caused due to the use of a more advanced data assimilation system in ERA5 (Cycle 31r2) than ERA-I (Cycle 41r2).

As obtained the wave model was forced with the ERA5 wind fields, the wave results obtained using CFSR wind fields exhibited similar behavior. In the statistical error results (Tables 3, 4), the RMSE and SI index significantly increase when the reducing C_{ds} from the value of 1.5, and similar increasing statistical error results were observed when the increasing C_{ds} from the value of 1.5. In general, CFSR slightly overestimated the wave data measured at

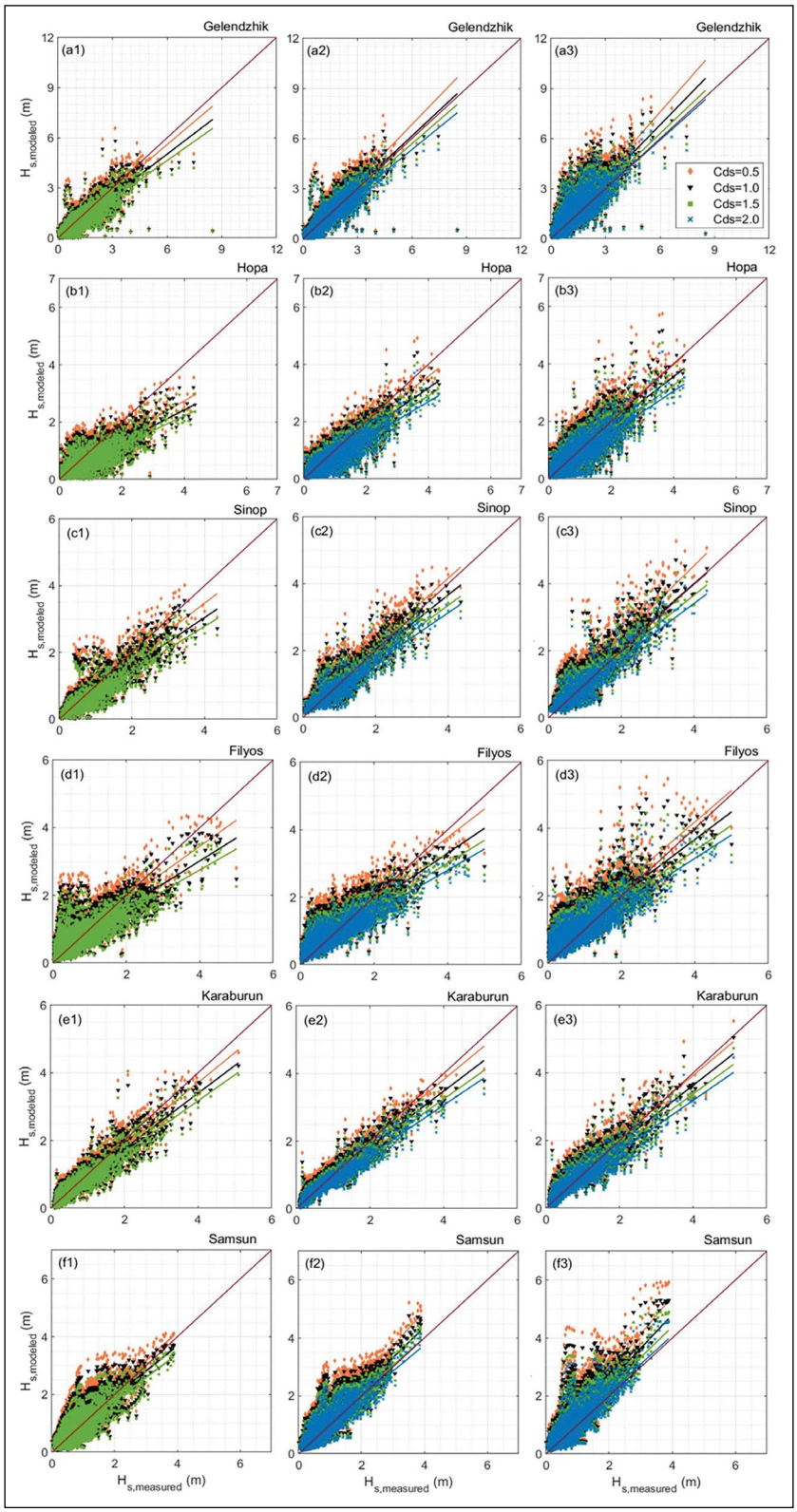

Figure 3. Scatter diagrams of the modeled significant wave height obtained using C_{ds}=0.5-2.0 against measured significant wave height at Gelendzhik, Hopa, Sinop, Filyos, Karaburun, and Samsun stations. Plots numbered 1, 2, and 3 represent the results for ERA-I, ERA5, and CFSR wind fields, respectively.

ERA-I: ERA-Interim; CFSR: Climate Forecast System Reanalysis.

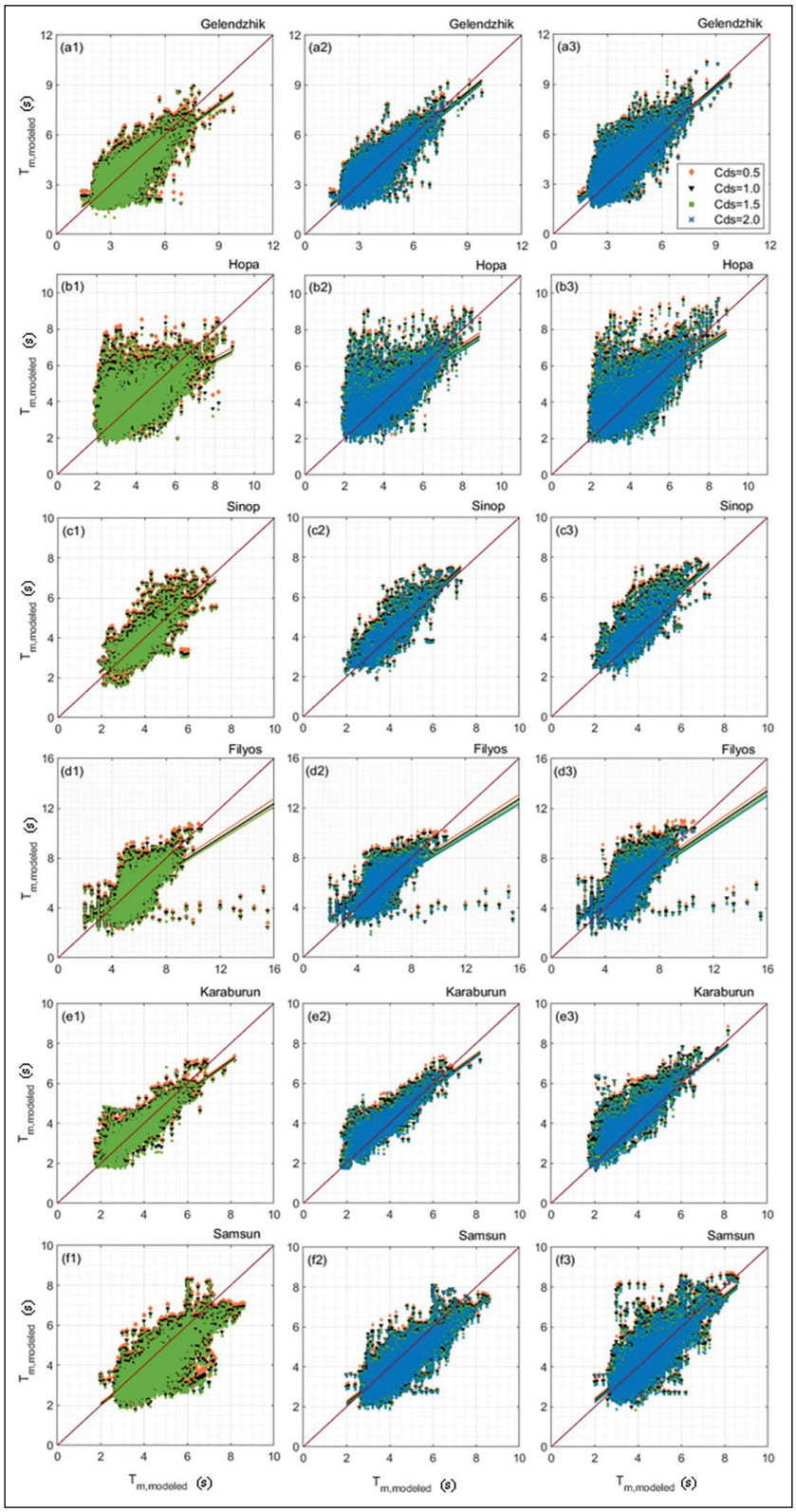

Figure 4. Scatter diagrams of the modeled wave period obtained using C_{ds}=0.5-2.0 against measured wave period at Gelendzhik, Hopa, Sinop, Filyos, Karaburun, and Samsun stations. Plots numbered 1, 2, and 3 represent the results for ERA-I, ERA5, and CFSR wind fields, respectively.

ERA-I: ERA-Interim; CFSR: Climate Forecast System Reanalysis.

Table 3. Statistical analysis of modeled significant wave heights using C_{ds} values ranging from 0.5 to 2.0 versus measured significant wave heights

		$H_{s,\ ERA\text{-}I}$ (m)			$H_{s,\ ERA5}$ (m)				$H_{s,\ CFSR}$ (m)			
	Measured	**C_{ds}=0.5**	**C_{ds}=1.0**	**C_{ds}=1.5**	**C_{ds}=0.5**	**C_{ds}=1.0**	**C_{ds}=1.5**	**C_{ds}=2.0**	**C_{ds}=0.5**	**C_{ds}=1.0**	**C_{ds}=1.5**	**Cds=2.0**
	Gelendzhik (1996–2003)											
Mean	0.723	0.734	0.640	0.584	0.903	0.788	0.719	0.669	1.044	0.914	0.834	0.777
Bias		0.010	-0.084	-0.140	0.180	0.065	-0.005	-0.054	0.321	0.191	0.111	0.054
RMSE		0.302	0.302	0.323	0.364	0.283	0.259	0.259	0.586	0.472	0.412	0.379
SI		0.418	0.417	0.446	0.503	0.391	0.358	0.359	0.810	0.652	0.570	0.524
R		0.896	0.896	0.896	0.924	0.924	0.923	0.922	0.867	0.864	0.863	0.861
	Hopa (1994–1999)											
Mean	0.560	0.576	0.501	0.453	0.677	0.585	0.528	0.487	0.774	0.668	0.602	0.555
Bias		0.017	-0.058	-0.106	0.118	0.026	-0.032	-0.073	0.214	0.108	0.043	-0.005
RMSE		0.306	0.317	0.336	0.262	0.238	0.247	0.264	0.362	0.299	0.277	0.273
SI		0.547	0.566	0.600	0.469	0.425	0.441	0.471	0.648	0.534	0.495	0.488
R		0.796	0.792	0.790	0.888	0.884	0.881	0.877	0.852	0.847	0.844	0.842
	Sinop (1994–1996)											
Mean	0.918	0.916	0.793	0.717	1.148	1.001	0.909	0.843	1.246	1.082	0.980	0.907
Bias		-0.002	-0.125	-0.201	0.229	0.082	-0.009	-0.076	0.327	0.164	0.062	-0.011
RMSE		0.345	0.356	0.391	0.375	0.286	0.272	0.287	0.499	0.367	0.315	0.301
SI		0.375	0.388	0.426	0.409	0.312	0.297	0.313	0.543	0.399	0.343	0.328
R		0.854	0.857	0.858	0.905	0.907	0.908	0.908	0.880	0.883	0.884	0.885
	Filyos (1994–1996)											
Mean	0.620	0.827	0.718	0.650	0.932	0.808	0.731	0.675	1.035	0.900	0.815	0.754
Bias		0.207	0.098	0.031	0.312	0.188	0.111	0.055	0.416	0.280	0.196	0.134
RMSE		0.390	0.339	0.330	0.414	0.328	0.297	0.290	0.529	0.412	0.355	0.326
SI		0.629	0.547	0.533	0.669	0.529	0.479	0.468	0.853	0.665	0.573	0.527
R		0.832	0.832	0.832	0.887	0.891	0.893	0.894	0.860	0.861	0.863	0.863
	Karaburun (2003–2004)											
Mean	0.784	0.849	0.757	0.700	0.920	0.815	0.748	0.699	1.006	0.893	0.819	0.765
Bias		0.065	-0.026	-0.084	0.137	0.032	-0.035	-0.084	0.222	0.109	0.035	-0.019
RMSE		0.245	0.243	0.267	0.229	0.197	0.213	0.240	0.336	0.270	0.255	0.261
SI		0.313	0.310	0.340	0.293	0.252	0.272	0.306	0.428	0.345	0.326	0.333
R		0.932	0.931	0.927	0.960	0.960	0.959	0.958	0.925	0.926	0.925	0.924
	Samsun (2016–2018)											
Mean	0.604	0.807	0.708	0.645	0.934	0.820	0.747	0.694	1.006	0.877	0.796	0.736
Bias		0.202	0.103	0.041	0.330	0.215	0.143	0.089	0.402	0.273	0.191	0.132
RMSE		0.364	0.291	0.262	0.433	0.320	0.259	0.224	0.549	0.411	0.332	0.281
SI		0.602	0.481	0.433	0.717	0.529	0.428	0.371	0.908	0.680	0.548	0.466
R		0.837	0.840	0.843	0.898	0.901	0.903	0.903	0.871	0.876	0.879	0.881

ERA-I: ERA-Interim; CFSR: Climate Forecast System Reanalysis; RMSE: Root Mean Square Error; SI: Scatter Index; R: Correlation coefficient.

almost all stations compared to wave results obtained with ERA5 and CFSR wind fields (Figs. 3, 4).

The following results were obtained from the scatter and Q-Q plot for significant wave heights and wave periods:

- There was found a good performance between modeled and measured significant wave heights up to 4 m at Gelendzhik station. However, the modeled significant wave heights were more scattered for higher wave height classes (exceeding 4 m). In higher percentiles, the significant wave height; (i) was underestimated when the increasing C_{ds} from the value of 0.5 for ERA-I, (ii) was underestimated when the increasing C_{ds} from the value of 1.5 for ERA-5, (iii) was overestimated when the decreasing C_{ds} from the value of 1.5 for CFSR (Fig. 3a, Appendix 1a).
- At Hopa station, (i) a better estimation of the significant wave height was obtained using C_{ds}=0.5 for ERA-I, (ii) the significant wave height was underestimated when the increasing C_{ds} from the value of 1.0 for ERA-5, (iii) modeled significant wave height gave more accurate results obtained using C_{ds}=1.5 for CFSR (Fig. 3b, Appendix 1b).
- At Sinop and Karaburun stations, in almost all wave height classes, more satisfactory model results were obtained using the value of C_{ds}=0.5 for ERA-I, C_{ds}=1.5 for both ERA5 and CFSR (Fig. 3c, e, Appendix 1c, e).
- At Filyos station, the measured and modeled significant wave height was reasonably well matched up to 2 m. In higher percentiles, the significant wave height, (i) was underestimated when the increasing C_{ds} from the value of 0.5 for ERA-I, (ii) was underestimated when the increasing C_{ds} from the value of 0.5 for ERA-5, (iii) overestimated when the decreasing C_{ds} from the value of 1.5 for CFSR (Fig. 3d, Appendix 1d).
- At Samsun station, modeled significant wave heights showed a good performance up to 3 m. However, the modeled wave results were more scattered in higher percentiles (exceeding 3 m). For higher wave

Table 4. Statistical analysis of modeled wave period using C_{ds} values ranging from 0.5 to 2.0 versus measured wave period

		$T_{m, ERA-I}$ (s)			$T_{m, ERA5}$ (s)				$T_{m, CFSR}$ (s)			
	Measured	C_{ds}=0.5	C_{ds}=1.0	C_{ds}=1.5	C_{ds}=0.5	C_{ds}=1.0	C_{ds}=1.5	C_{ds}=2.0	C_{ds}=0.5	C_{ds}=1.0	C_{ds}=1.5	Cds=2.0
	Gelendzhik (1996–2003)											
Mean	3.511	3.532	3.398	3.316	3.794	3.664	3.580	3.517	4.020	3.889	3.803	3.737
Bias		0.020	-0.114	-0.196	0.283	0.153	0.070	0.006	0.509	0.378	0.293	0.227
RMSE		0.602	0.623	0.650	0.604	0.563	0.552	0.553	0.859	0.800	0.768	0.747
SI		0.171	0.177	0.185	0.172	0.160	0.157	0.157	0.245	0.228	0.219	0.213
R		0.826	0.822	0.814	0.868	0.867	0.864	0.861	0.805	0.802	0.800	0.799
	Hopa (1994–1999)											
Mean	3.896	4.149	4.004	3.906	4.375	4.241	4.150	4.079	4.431	4.277	4.175	4.095
Bias		0.253	0.108	0.010	0.479	0.345	0.254	0.183	0.535	0.381	0.279	0.199
RMSE		0.973	0.950	0.946	0.946	0.898	0.874	0.862	1.020	0.951	0.914	0.891
SI		0.250	0.244	0.243	0.243	0.230	0.224	0.221	0.262	0.244	0.235	0.229
R		0.612	0.606	0.602	0.718	0.709	0.704	0.700	0.699	0.698	0.698	0.699
	Sinop (1994–1996)											
Mean	3.955	4.127	4.026	3.954	4.379	4.282	4.210	4.149	4.597	4.488	4.407	4.341
Bias		0.172	0.071	-0.001	0.425	0.328	0.255	0.195	0.642	0.534	0.452	0.386
RMSE		0.671	0.650	0.645	0.695	0.636	0.599	0.575	0.923	0.847	0.793	0.755
SI		0.170	0.164	0.163	0.176	0.161	0.151	0.145	0.233	0.214	0.201	0.191
R		0.771	0.769	0.767	0.841	0.843	0.843	0.843	0.787	0.789	0.789	0.789
	Karaburun (2003–2004)											
Mean	3.687	3.902	3.784	3.703	4.181	4.064	3.981	3.917	4.387	4.265	4.175	4.104
Bias		0.215	0.097	0.015	0.494	0.377	0.294	0.230	0.700	0.578	0.488	0.416
RMSE		0.543	0.530	0.535	0.674	0.598	0.554	0.528	0.890	0.809	0.753	0.715
SI		0.147	0.144	0.145	0.183	0.162	0.150	0.143	0.241	0.219	0.204	0.194
R		0.857	0.844	0.837	0.879	0.876	0.873	0.871	0.832	0.826	0.824	0.822
	Samsun (2016–2018)											
Mean	4.342	3.951	3.834	3.749	4.222	4.119	4.044	3.983	4.482	4.383	4.307	4.244
Bias		-0.390	-0.508	-0.593	-0.120	-0.223	-0.298	-0.359	0.140	0.041	-0.035	-0.098
RMSE		0.786	0.858	0.917	0.590	0.621	0.655	0.688	0.714	0.698	0.696	0.701
SI		0.181	0.198	0.211	0.136	0.143	0.151	0.159	0.164	0.161	0.160	0.161
R		0.771	0.762	0.754	0.834	0.832	0.829	0.826	0.787	0.789	0.789	0.789
		$T_{p, ERA-I}$ (s)			$T_{p, ERA5}$ (s)				$T_{p, CFSR}$ (s)			
	Filyos (1995–1996)											
Mean	5.491	5.341	5.180	5.067	5.695	5.535	5.424	5.335	5.855	5.681	5.555	5.455
Bias		-0.150	-0.311	-0.424	0.204	0.044	-0.067	-0.156	0.365	0.190	0.064	-0.036
RMSE		1.057	1.079	1.109	1.009	0.980	0.975	0.983	1.138	1.080	1.055	1.047
SI		0.192	0.196	0.202	0.184	0.178	0.178	0.179	0.207	0.197	0.192	0.191
R		0.654	0.652	0.651	0.677	0.675	0.674	0.672	0.659	0.658	0.659	0.659

ERA-I: ERA-Interim; CFSR: Climate Forecast System Reanalysis; RMSE: Root Mean Square Error; SI: Scatter Index; R: Correlation coefficient.

Table 5. Statistical analysis of modeled significant wave height and wave period at Bosphorus station

	Mean (m)	Bias (m)	RMSE (m)	SI	R	Mean (s)	Bias (s)	RMSE (s)	SI	R
	Bosphorus (2016-2018)									
	H_s					T_p				
Measured	0.789					4.879				
ERA-I	0.998	0.245	0.411	0.520	0.906	5.329	0.451	1.192	0.244	0.710
ERA5	0.975	0.185	0.291	0.369	0.946	5.326	0.446	1.120	0.230	0.739
CFSR	0.982	0.193	0.367	0.465	0.920	5.544	0.665	1.304	0.267	0.737

RMSE: Root Mean Square Error; SI: Scatter Index; R: Correlation coefficient; ERA-I: ERA-Interim; CFSR: Climate Forecast System Reanalysis.

height classes, the significant wave height; (i) was underestimated when the increasing C_{ds} from the value of 1.0 for ERA-I, (ii) overestimated when the increasing C_{ds} from the value of 1.0 for ERA-5, (iii) overestimated when the decreasing C_{ds} from the value of 2.0 for CFSR (Fig. 3f, Appendix 1f).

- Although the scatter diagrams and Q-Q plots for the wave periods were quite similar, ERA-5 and CFSR have slightly better performance in the prediction of the wave periods modeled with the value of C_{ds}=1.5 than those obtained using C_{ds}=0.5 for ERA-I (Fig. 4, Appendix 2, Table 4).

In considering all measurement stations and results of several statistical investigations, the best performance between the modeled and measured significant wave heights and wave periods were obtained using the value of C_{ds}=0.5 for the ERA-I, and 1.5 for both ERA5 and CFSR. The wave results obtained using ERA5 and CFSR wind fields showed a relatively better agreement with wave measurements than

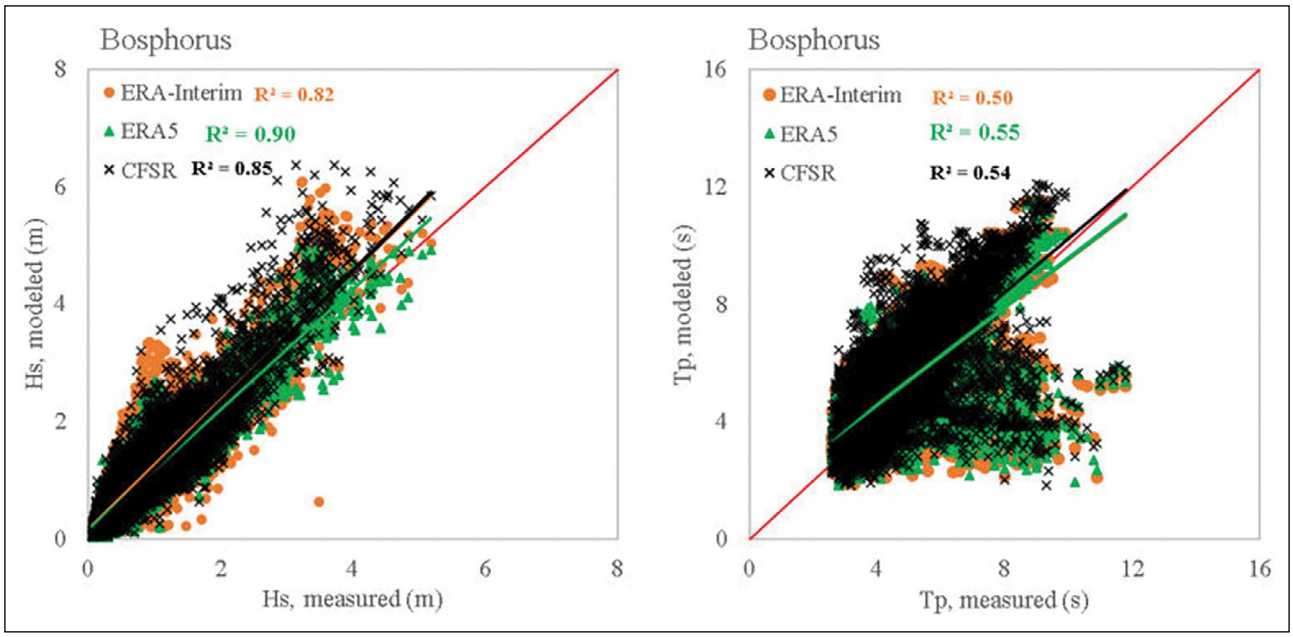

Figure 5. Validation of the calibrated MIKE 21 SW model results against the measurements for significant wave heights and peak wave periods at the Bosphorus station.
CFSR: Climate Forecast System Reanalysis.

wave results modeled using ERA-I wind fields. Although both ERA5 and CFSR were satisfactorily good performance in the prediction of the Black Sea wave climate, ERA5 provided slightly better performance than the CFSR. Results show that ERA5 has large correlation coefficients and low errors, i.e., ERA5 provides a better representation of the wave climate in the Black Sea.

4.2. Validation evaluation in the Black Sea

After the calibration processes, the model results were verified at another measurement station. The validation of the calibrated MIKE 21 SW model was conducted with the wave measurements at the Bosphorus station (Fig. 2, Table 2). The statistical error results are summarized in Table 5, the scatter plots are shown in Figure 5, and the comparisons of the time histories between the modeled and measured significant wave heights and peak wave periods are shown in Figure 6.

In general, modeled significant wave heights and peak wave periods obtained using three different wind sources are in reasonably good agreement with wave measurements at the Bosphorus station (Fig. 5). By referring to Figures 5 and 6, and Table 5, the modeled wave results using ERA5 gave more accurate results compared to those obtained with ERA-I and CFSR. For example, the largest correlation coefficient (R) was determined for the wave model forced with ERA5 wind fields and followed by CFSR, and ERA-I. Moreover, modeled wave results obtained using ERA5 wind fields have the lowest bias, RMSE, and SI compared to the results for CFSR, and ERA-I. The scatter diagram shows the relationship between the modeled and measured significant wave heights and wave periods. From Figure 5, modeled wave results obtained for ERA-5 exhibit less scattering compared to those obtained with ERA-I and CFSR. A slight overestimation of significant wave height is detected for both ERA-I and CFSR, and more accurate wave results are determined for ERA5. These results imply that ERA5 provides better model performance in the prediction of the Black Sea wave properties than CFSR and ERA-I.

The comparative time series plots between modeled and measured significant wave heights and peak wave periods at the Bosphorus station are presented in Figure 6. A relatively good agreement was observed between the wave results modeled using three wind sources and measured wave results. However, ERA-I slightly lower performed in predicting significant wave heights and peak wave periods than those obtained with ERA-5 and CFSR.

It is important to note that wave results modeled using ERA5 were a slightly better performance compared to wave results for CFSR and ERA-I.

5. CONCLUSIONS

In the study, the performance of MIKE 21 SW forced with the three different reanalysis wind fields, namely ERA-I, ERA5, and CFSR, were evaluated to determine the better predictions of the wave climate in the Black Sea. The spectral wave model was calibrated and validated with wave measurements at seven different locations along the Black Sea to determine the optimal model settings. The model

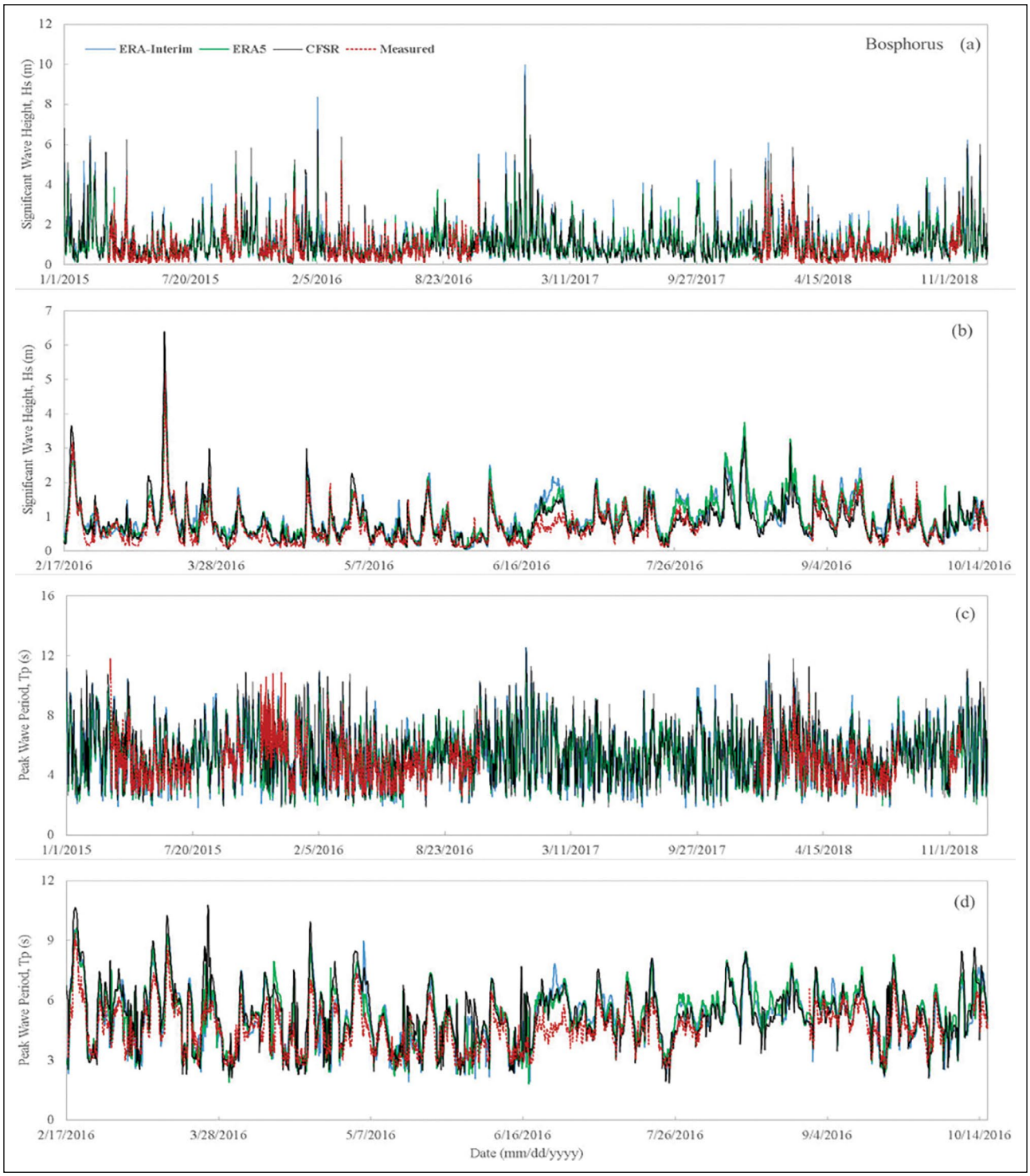

Figure 6. Comparison between measured and modeled significant wave heights and peak wave periods (a, c) all measurement time, (b, d) closer examination at Bosphorus station.

CFSR: Climate Forecast System Reanalysis.

simulations performed by varying different physical model parameters showed a strong sensitivity to the whitecapping parameter (C_{ds}) and did not show sensitivity to the parameters such as bottom friction (k_n), depth-induced wave breaking (γ), and nonlinear wave-wave interactions.

In the Black Sea basin, the following model settings gave more accurate results: (i) the wind input was computed based on the formulation of Komen et al. (1994), (ii) the formulation of Komen et al. (1994) was considered for the dissipation due to whitecapping and the values of C_{ds}=0.5

for ERA-I wind fields, and C_{ds}=1.5 for both ERA5 and CFSR wind fields, (iii) constant Nikuradese roughness (k_n=0.04 m) was used for the bottom friction dissipation, (iv) the formulation for the dissipation due to depth induced wave breaking (α=1, γ=0.8) was based on the bore model of Battjes and Janssen (1978), (iv) quadruplet wave interactions were estimated in the simulations using the DIA by proposed Hasselman et al. (1985).

The calibrated MIKE 21 SW model was validated against wave measurements obtained from Bosphorus station. Our analyses indicate that wind sources are one of the most important parameters affecting the model performance in the prediction of the Black Sea wave properties. According to the statistical error measures and comparative analyses, the largest correlation coefficient (R) and relatively low statistical error results (bias, RMSE, SI) were detected by the wave model forced with ERA5 wind fields, followed by the wave results obtained using CFSR, and ERA-I wind fields. In general, the wave results modeled using ERA-I wind fields were lower performed in predicting significant wave heights and wave periods compared to wave results obtained with ERA5 and CFSR wind fields. Moreover, ERA-I provided less accurate wave results than those obtained with ERA5 and CFSR wind fields. Although minor differences were obtained in the wave results modeled between ERA5 and CFSR, the ERA5 showed slightly better performance in the prediction of the Black Sea wave properties.

There could be many reasons for minor differences in wave results modeled using different wind fields. The wave results modeled using wind fields strongly depend on the wind speed. Therefore, a small variation in wind speeds can result in a change in modeled wave parameters. Previous studies reported that ERA-I slightly underestimated the wind speed compared to CFSR. Another possible reason may be the effect of different spatial and temporal resolutions of wind fields on wave model performance. Many innovative improvements made to ECMWF ERA5 (e.g., a more advanced assimilation system, a significantly increased horizontal resolution, higher temporal resolution, uncertainty estimate) resulted in better model performance than those obtained with ECMWF ERA-I.

DATA AVAILABILITY STATEMENT

The published publication includes all graphics and data collected or developed during the study.

CONFLICT OF INTEREST

The author declared no potential conflicts of interest with respect to the research, authorship, and/or publication of this article.

ETHICS

There are no ethical issues with the publication of this manuscript.

FINANCIAL DISCLOSURE

The authors declared that this study has received no financial support.

REFERENCES

Akpinar, A., Ponce de Le´on, S., (2016). An assessment of the wind re-analyses in the modelling of an extreme sea state in the Black Sea. Dynamics of Atmospheres and Oceans, 73, 61–75. [CrossRef]

Ari Guner, H. A., Yuksel, Y., and Ozkan Cevik, E. (2013). Estimation of wave parameters based on nearshore wind–wave correlations. Ocean Engineering, 63, 52–62. [CrossRef]

Battjes, J.A., Janssen, J.P.F.M. (1978). Energy loss and set-up due to breaking of random waves Proceedings of the 16th Conference on Coastal Engineering, ASCE, Hamburg, Germany, 569–587. [CrossRef]

Cavaleri, L., Bertotti, L. (2005). The improvement of modeled wind and wave fields with increasing resolution. Ocean Engineering, 33, 553–565. [CrossRef]

Cavaleri, L., Abdalla, S., Benetazzo, A., Bertotti, L., Bidlot, J.R., Breivik, O., et al. (2018). Wave modelling in coastal and inner seas. Progress in Oceanography, 167, 164–263. [CrossRef]

Dee, D.P., Uppala, S.M., Simmons, A.J., Berrisford, P., Poli, P., Kobayashi, S., Andrae, U., Balmaseda, M.A., Balsamo, G., Bauer, P., Bechtold, P., Beljaars, A.C.M., van de Berg, L., Bidlot, J., Bormann, N., Delsol, C., Dragani, R., Fuentes, M., Geer, A.J., Haimberger, L., Healy, S.B., Hersbach, H., Holm, E.V., Isaksen, L., Kallberg, P., Kohler, M., Matricardi, M., McNally, A.P., Monge-Sanz, B.M., Morcrette, J.J., Park, B.K., Peubey, C., de Rosnay, P., Tavolato, C., Thepaut, J.N., Vitart, F. (2011). The ERA-interim reanalysis configuration and performance of the data assimilation system. Quarterly Journal of the Royal Meteorological Society, 137, 553–597. [CrossRef]

DHI (2007). MIKE 21 - Spectral wave module - Scientific Document, 42. https://manuals.mikepoweredbydhi.help/2017/Coast_and_Sea/M21SW_Scientific_Doc.pdf

Divinsky, B.V., Kosyan, R.D. (2015). Observed wave climate trends in the offshore Black Sea from 1990 to 2014. Oceanology, 55, 837–843. [CrossRef]

Divinsky, B.V., Kosyan, R.D. (2017). Spatiotemporal variability of the Black Sea wave climate in the last 37 years. Continental Shelf Research, 136, 1–19. [CrossRef]

DLH, (1999). Port hydraulics laboratory filyos harbour wave measurements.

Hasselmann, S., Hasselmann, K., Allender, J. H., Barnett, T. P., (1985). Computations and parameterizations

of the nonlinear energy transfer in a gravity-wave spectrum. Part II: Parameterizations of the nonlinear energy transfer for application in wave models.
Journal of Physical Oceanography, 15, 1378–1391. [CrossRef]
Hersbach, H., Dee, D. (2016). ERA5 reanalysis is in production, ECMWF Newsletter, 147, 7.
Holthuijsen, L., Booij, N., & Herbers, T. (1989). A prediction model for stationary, short-crested waves in shallow water with ambient currents. Coastal Engineering, 13, 23–54. [CrossRef]
Islek, F., Yuksel, Y., Sahin, C. (2020a). Spatiotemporal long-term trends of extreme wind characteristics over the Black Sea. Dynamics of Atmospheres and Oceans, 90, Article 101132. [CrossRef]
Islek, F., Yusek Y., and Sahin C., (2020b). Assessments of long-term wind and wave trends in the Black Sea. Proceedings of virtual Conference on Coastal Engineering. [CrossRef]
Islek, F., Yuksel, Y., Sahin, C., Ari Guner, H.A. (2021). Long-term analysis of extreme wave characteristics based on the SWAN hindcasts over the Black Sea. Dynamics of Atmospheres and Oceans, 94, Article 101165. [CrossRef]
Islek, F., and Yuksel, Y. (2021). Inter-comparison of long-term wave power potential in the Black Sea based on the SWAN wave model forced with two different wind fields. Dynamics of Atmospheres and Oceans, 93, Article 101192. [CrossRef]
Komen, G.J., Cavaleri, L., Donelan, M., Hasselmann, K., Hasselmann, S., Janssen P.A.E.M. (1994). Dynamics and modelling of ocean waves, Cambridge University Press. [CrossRef]
Myslenkov, S.A., Shestakova, A.A., Toropov, P.A., (2016). Numerical simulation of storm waves near the northeastern coast of the Black Sea. Russian Meteorology and Hydrology, 41, 706–713. [CrossRef]
Myslenkov, S.A., Zelenko, A., Resnyanskii, Y., Arkhipkin, V., and Silvestrova K. (2021). Quality of the wind wave forecast in the Black Sea including storm wave analysis. Sustainability, 13(23), Article 13099. [CrossRef]
Onea, F., Raileanu, A., Rusu, E. (2015). Evaluation of the Wind Energy Potential in the Coastal Environment of two Enclosed Seas. Advances in Meteorology, 2015, Article 808617. [CrossRef]
Ozhan, E., and Abdalla, S. (2002). Wind and Deep Water Wave Atlas of Turkish Coasts, Turkish National Coastal Zone Management Committee/ MEDCOAST. Middle East Technical University, Ankara, pp. 445.
Rusu, L., Bernardino, M., Soares, C.G. (2014). Wind and wave modelling in the Black Sea. Journal of Operational Oceanography, 7(1), 5–20. [CrossRef]
Saha, S., Moorthi, S., Pan, H.-L., Wu, X., Wang, J., Nadigai, S., Tripp, P., Kistler, R., Woollen, J., Behringer, D., Liu, H., Stokes, D., Grumbine, R., Gayno, G., Wang, J., Hou, Y.-T., Chuang, H.-Y., Juang, H.-M.H., Sela, J., Iredell, M., Treadon, R., Kleist, D., van Delst, P., Keyser, D., Derber, J., Ek, M., Meng, J., Wei, H., Yang, R., Lord, S., van den Dool, H., Kumar, A., Wang, W., Long, C., Chelliah, M., Xue, Y., Huang, B., Schemm, J.-K., Ebisuzaki, W., Lin, R., Xie, P., Chen, M., Zhou, S., Higgins, W., Zou, C.-Z., Liu, Q., Chen, Y., Han, Y., Cucurull, L., Reynolds, R.W., Rutledge, G., & Goldberg, G. (2010). The NCEP climate forecast system reanalysis. Bulletin of the American Meteorological Society, 91, 1015–1057. [CrossRef]
Saha, S., Moorthi, S., Wu, X., Wang, J., Nadiga, S., Tripp, P., Behringer, D., Hou, Y.-T., Chuang, H., Iredell, M., Ek, M., Meng, J., Yang, R., Mendez, M.P., van den Dool, H., Zhang, Q., Wang, W., Chen, M., & Becker, E. (2014). The NCEP climate forecast system version 2. Journal of Climate, 27, 2185–2208. [CrossRef]
Soomere, T., & Räämet, A. (2011). Long-term spatial variations in the Baltic Sea wave fields. Ocean Science, 7(1), 141–150. [CrossRef]
Weisse, R., & von Storch, H. (2010). Marine Climate and Climate Change Storms, Wind Waves and Storm Surges. Springer, 200. [CrossRef]
Valchev, N., Davidan, I., Belberov, Z., Palazov, A., & Valcheva, N. (2010). Hindcasting and assessment of the western black sea wind and wave climate. Journal of Environmental Protection and Ecology, 11, 1001–1012.
Valchev, N.N., Andreeva, N.K., & Valcheva, N.N. (2013). Assessment of off-shore wave energy in the Black Sea on the basis of long-term wave hindcast. Developments in Maritime Transportation and Exploitation of Sea Resources, 1021–1028. [CrossRef]
Vledder, V., & Akpinar, A. (2015). Wave model predictions in the Black Sea: sensitivity to wind fields. Applied Ocean Research, 53, 161–178. [CrossRef]
Yuksel, Y., Yuksel, Z.T., & Sahin C. (2020). Effect of long-term wave climate variability on performance-based design of coastal structures. Aquatic Ecosystem Health & Management, 23(4), 407–416. [CrossRef]
Yuksel, Y., Yuksel, Z.T., Islek, F., Sahin C., & Ari Guner, H.A. (2021). Spatiotemporal long-term trends of wind and wave climate and extreme characteristics over the Sea of Marmara. Ocean Engineering, 228, Article 108946. [CrossRef]

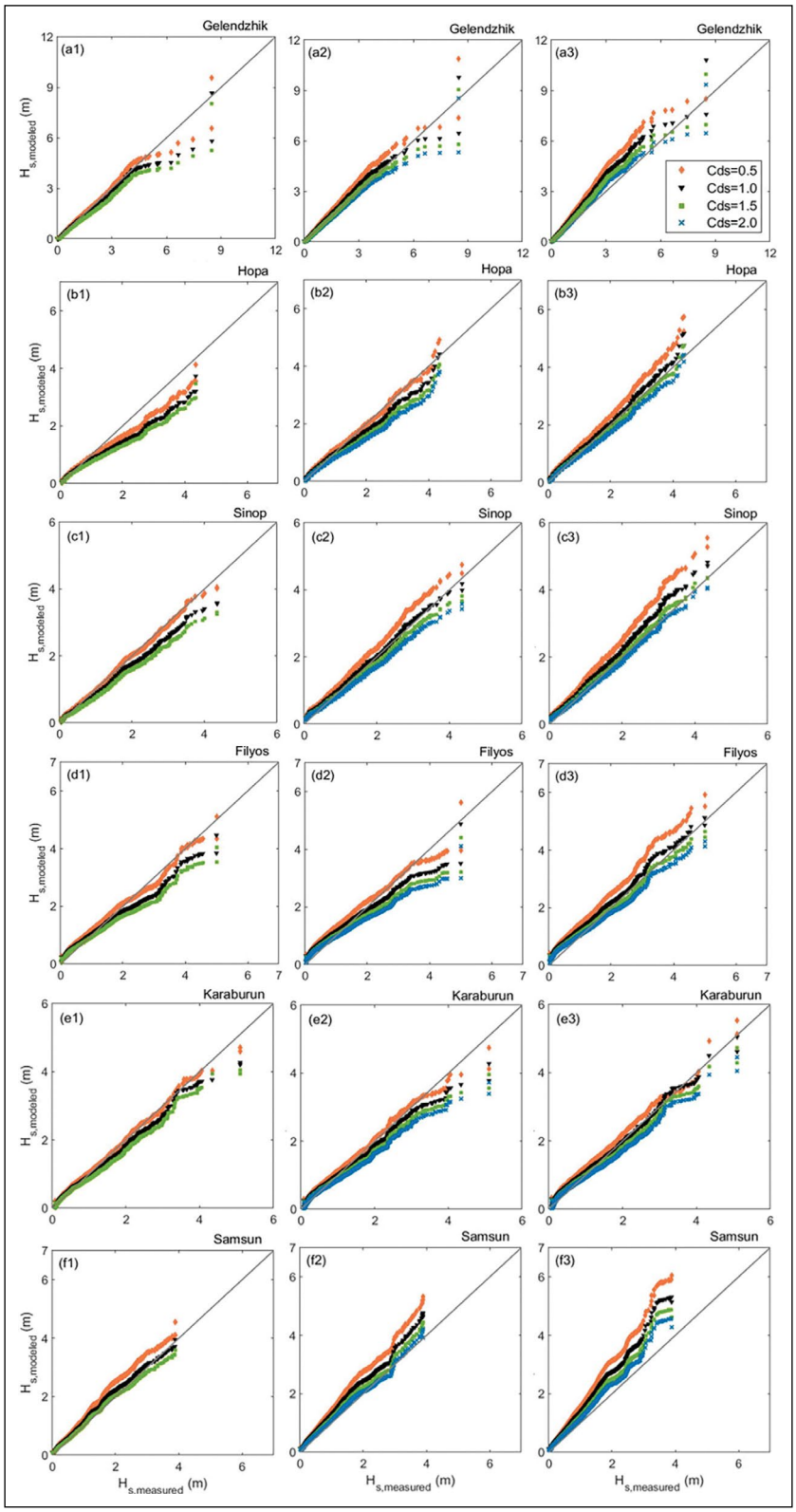

Appendix 1. Quantile-Quantile plots of significant wave height modeled using three wind fields against measured significant wave height at Gelendzhik, Hopa, Sinop, Filyos, Karaburun, and Samsun stations. Plots numbered 1, 2, and 3 represent the results for ERA-I, ERA5, and CFSR wind fields, respectively.

ERA-I: ERA-Interim; CFSR: Climate Forecast System Reanalysis.

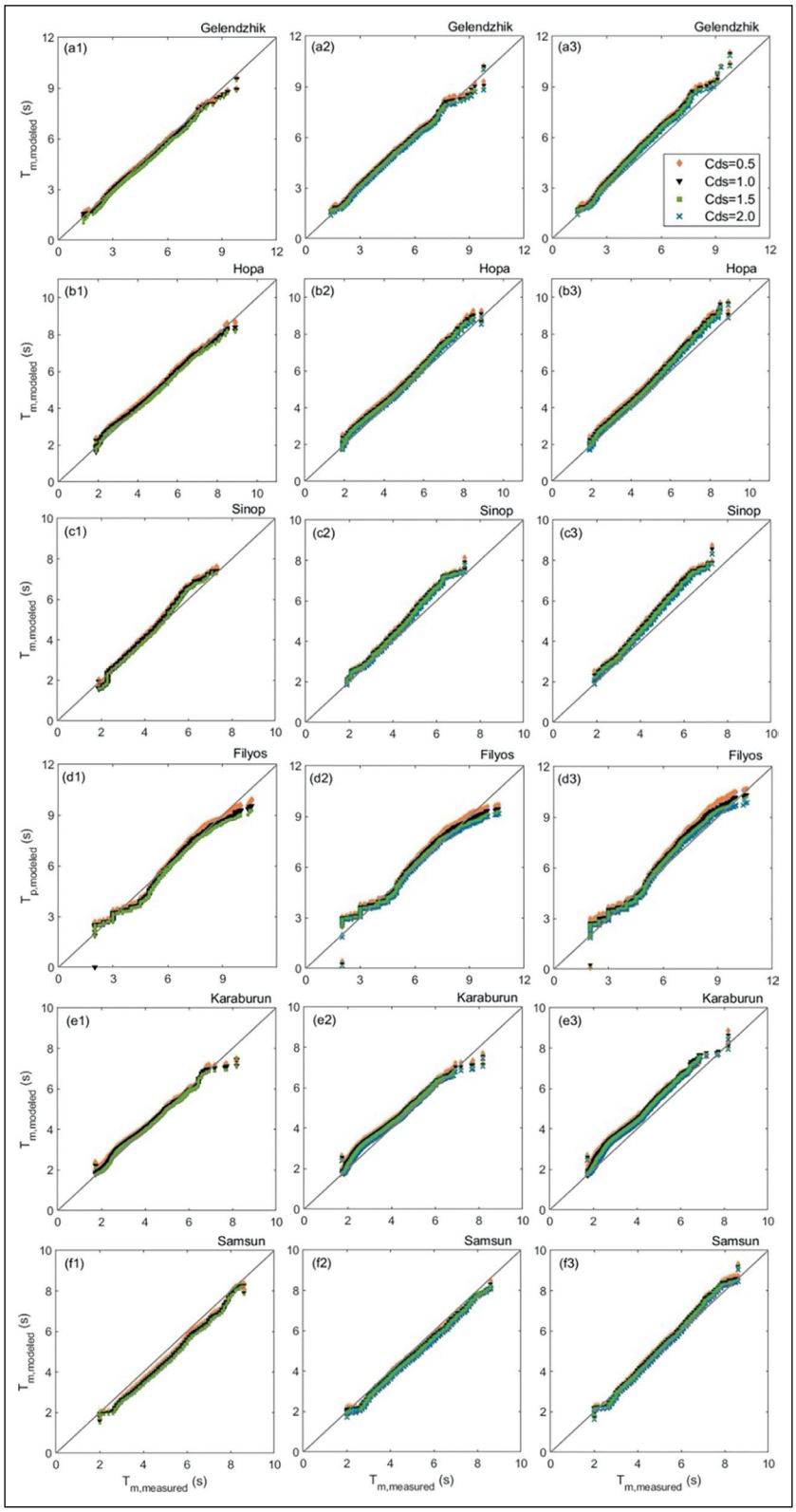

Appendix 2. Quantile-Quantile plots of wave period modeled using three reanalysis wind fields against measured wave period at Gelendzhik, Hopa, Sinop, Filyos, Karaburun, and Samsun stations. Plots numbered 1, 2, and 3 represent the results for ERA-I, ERA5, and CFSR wind fields, respectively.

ERA-I: ERA-Interim; CFSR: Climate Forecast System Reanalysis.

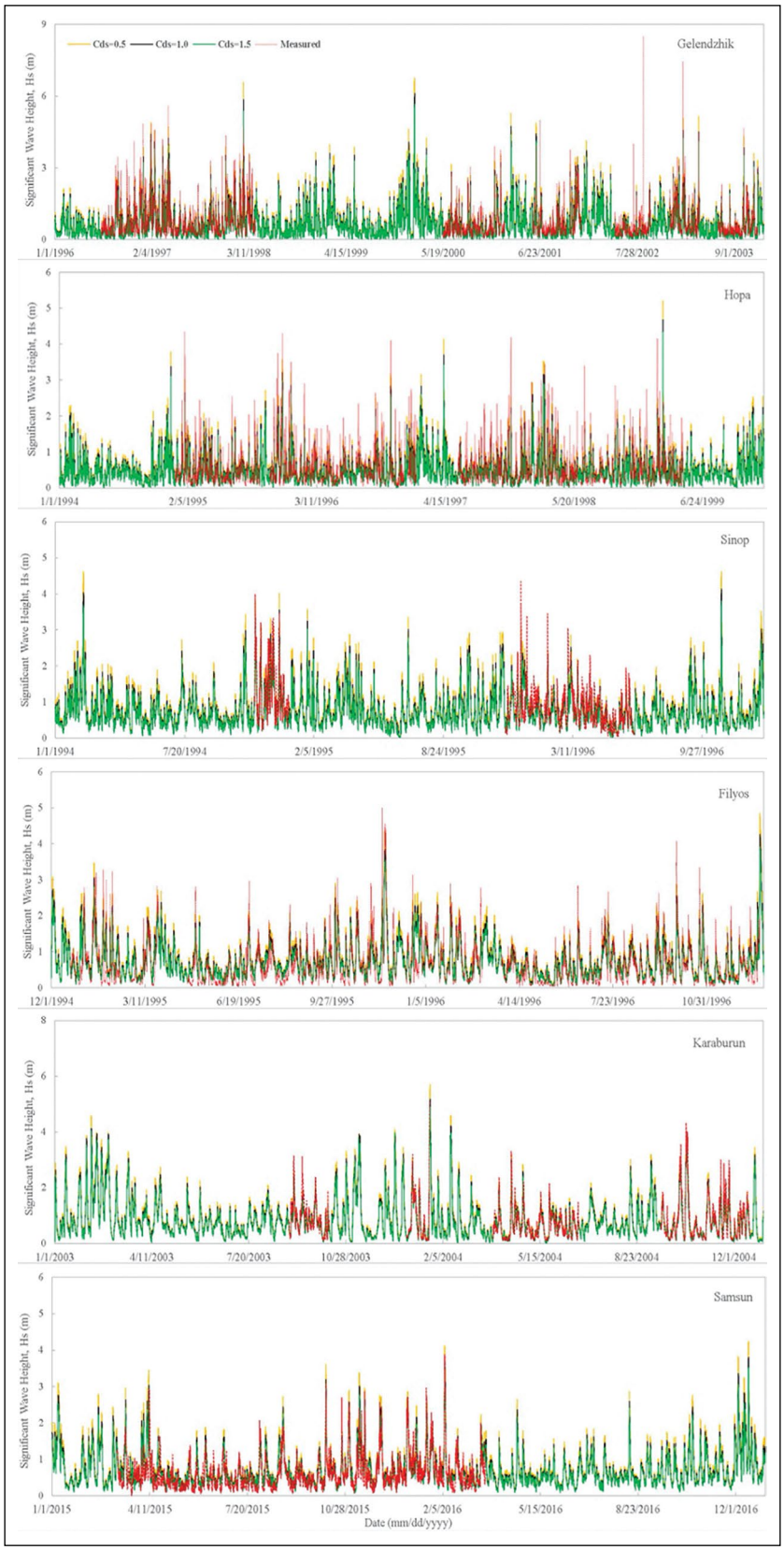

Appendix 3. Comparison between significant wave height modeled using ERA-Interim wind fields and measured at Gelendzhik, Hopa, Sinop, Filyos, Karaburun, and Samsun stations.

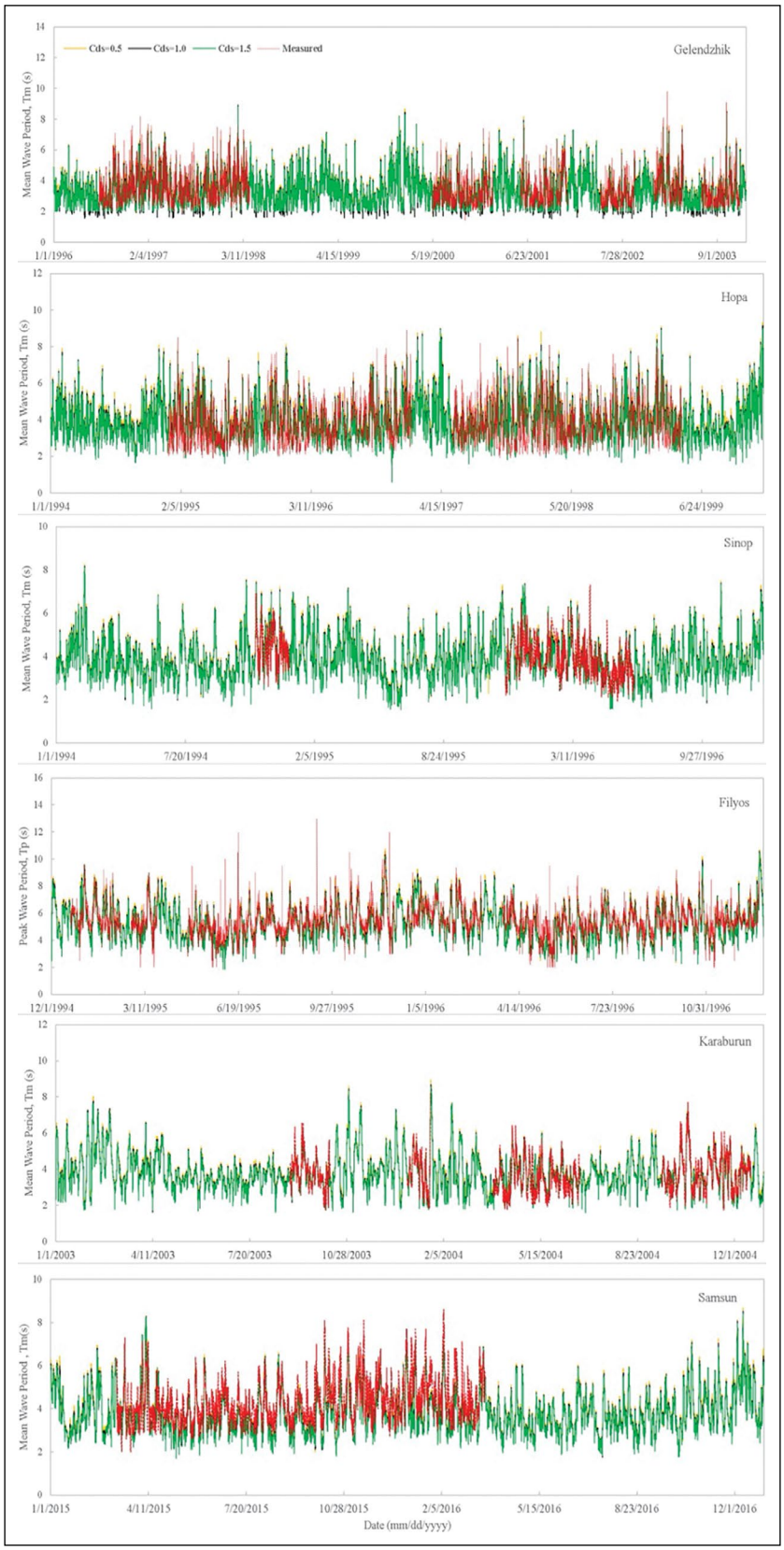

Appendix 4. Comparison between wave period modeled using ERA-Interim wind fields and measured at Gelendzhik, Hopa, Sinop, Filyos, Karaburun, and Samsun stations.

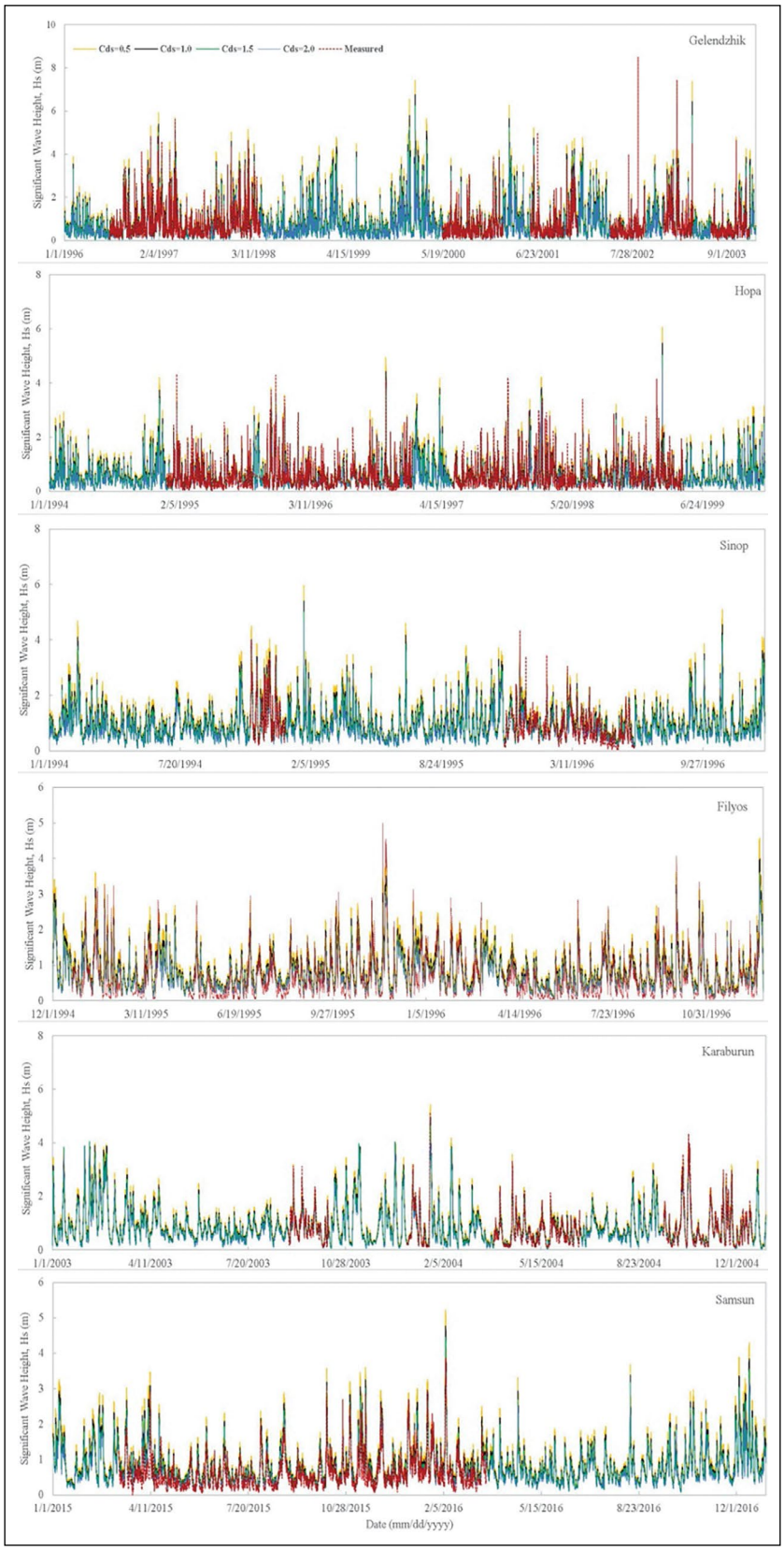

Appendix 5. Comparison between significant wave height modeled using ERA5 wind fields and measured at Gelendzhik, Hopa, Sinop, Filyos, Karaburun, and Samsun stations.

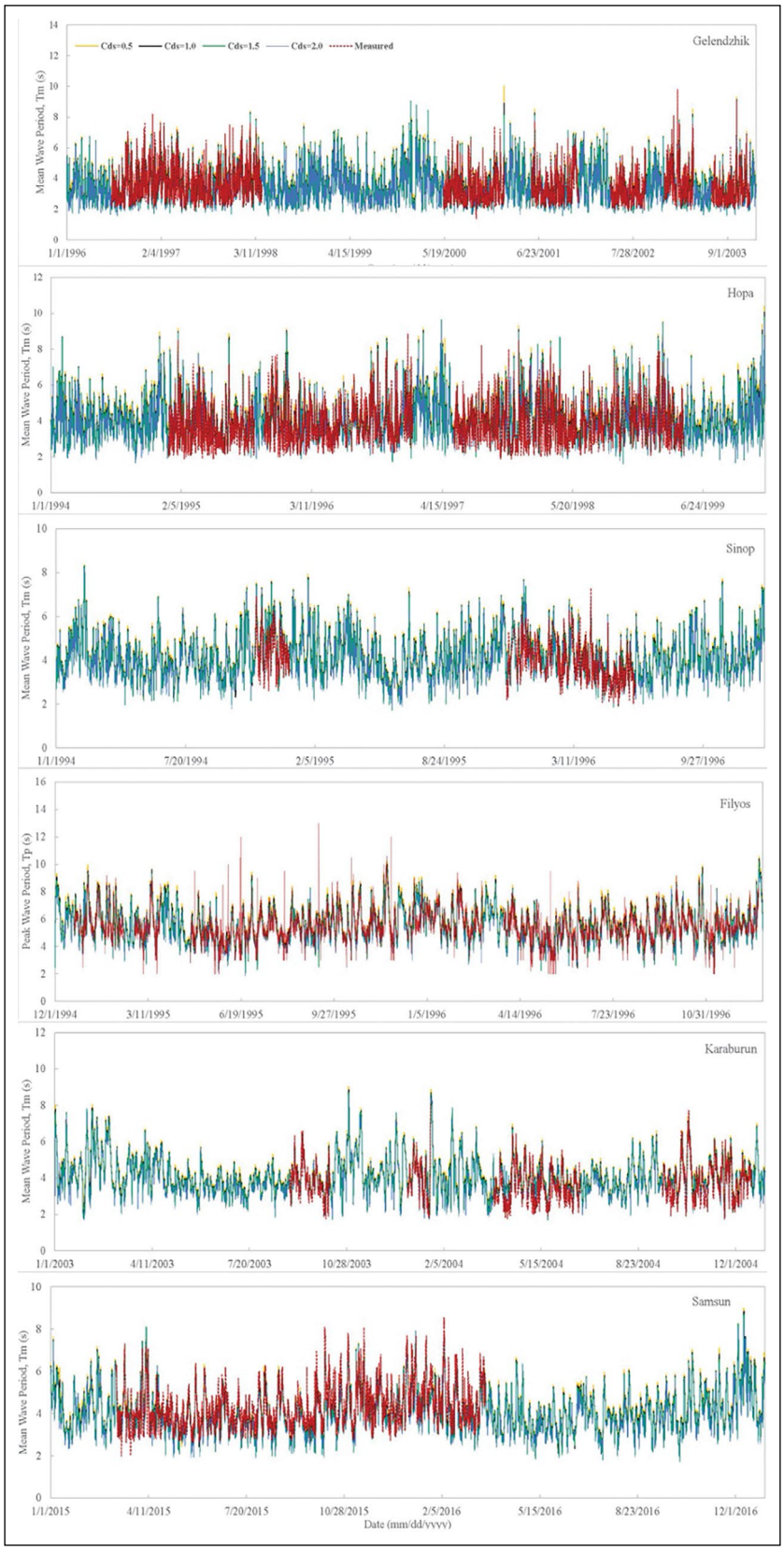

Appendix 6. Comparison between wave period modeled using ERA5 wind fields and measured at Gelendzhik, Hopa, Sinop, Filyos, Karaburun, and Samsun stations.

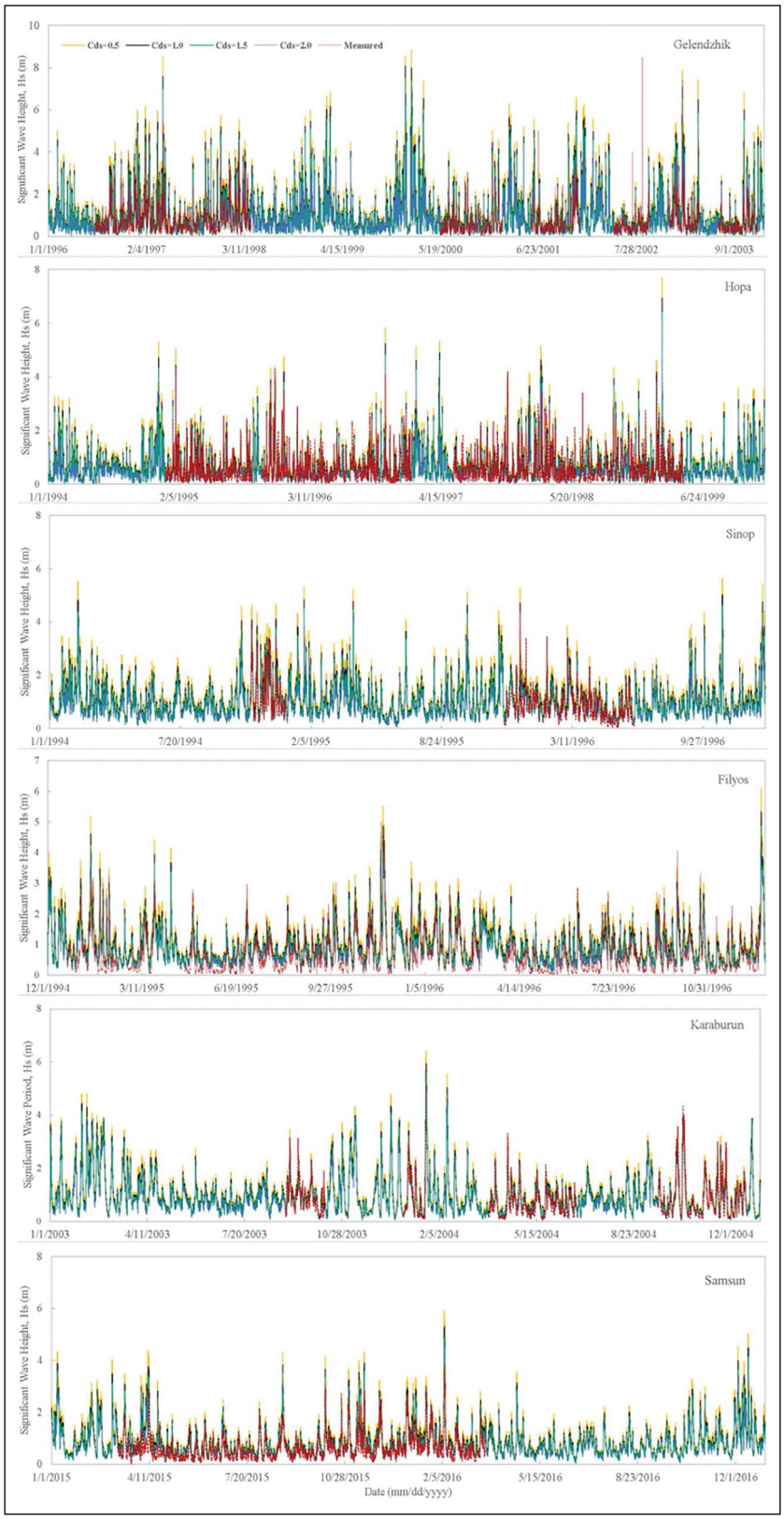

Appendix 7. Comparison between significant wave height modeled using CFSR wind fields and measured at Gelendzhik, Hopa, Sinop, Filyos, Karaburun, and Samsun stations.

CFSR: Climate Forecast System Reanalysis.

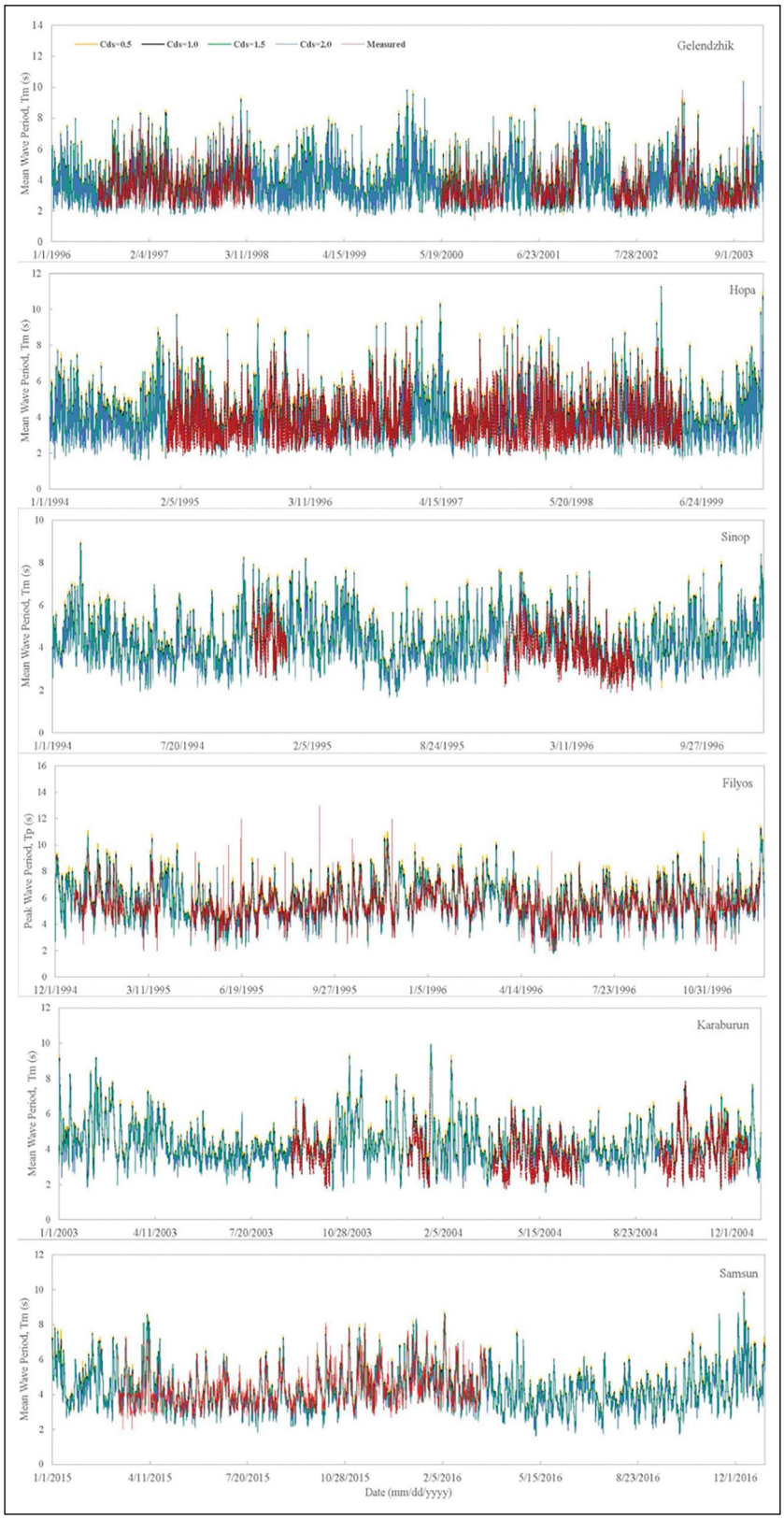

Appendix 8. Comparison between wave period modeled using CFSR wind fields and measured at Gelendzhik, Hopa, Sinop, Filyos, Karaburun, and Samsun stations.

CFSR: Climate Forecast System Reanalysis.